Stability of Jurkat cells during short-term liquid storage analyzed by flow imaging microscopy

Rösch, A.R.; Hiemenz, C.; Findley, T.; Goldberg, I.; Windisch, R.; Wichmann, C.; ... ; Menzen, T.

European Journal of Pharmaceutics and Biopharmaceutics 211 (2025) 114703

Contents lists available at ScienceDirect

European Journal of Pharmaceutics and Biopharmaceutics

journal homepage: www.elsevier.com/locate/ejpb

Research paper

Stability of Jurkat cells during short-term liquid storage analyzed by flow imaging microscopy

Alexandra Roesch [a,b], Cornelia Hiemenz [a], Teresa Findley [c], Ilya Goldberg [c], Roland Windisch [d], Christian Wichmann [d], Gideon Kersten [a,b], Tim Menzen [a,*]

[a] Coriolis Pharma, Fraunhoferstr. 18 b, 82152 Martinsried, Germany
[b] Leiden Academic Centre for Drug Research (LACDR), Leiden University, PO Box 9502, 2300 RA, Leiden, the Netherlands
[c] ViQi Inc., 315 Meigs Road, Suite A261, Santa Barbara, CA 93109, United States
[d] Division of Transfusion Medicine, Cell Therapeutics and Haemostaseology, University Hospital, LMU Munich, Munich, Germany

ARTICLE INFO

Keywords:
Cell-based medicinal products
Cell viability
Cell storage
Dimethyl sulfoxide
Stability

ABSTRACT

The viability of cell-based medicinal products (CBMPs) is a critical quality attribute and must be assessed throughout the product lifecycle to contribute to a safe and potent drug product. In this study, we investigated the impact of short-term liquid storage conditions, encountered during manufacturing of CBMPs, such as holding times outside cell culture conditions and medium composition, on cell viability.

As a model for T cells Jurkat cells were used and stored in different storage media for up to 24 h outside a freezer and outside of cell culture conditions. The effect of storage in different storage media, i.e., cell culture medium or phosphate buffered saline (PBS), dimethyl sulfoxide (DMSO) at different storage temperatures as well as the impact of pH on the cell viability was assessed. The viability of the cells was assessed by (i) flow cytometry with an Annexin V and CalceinAM staining or (ii) machine learning tools, leveraging the morphological information of flow imaging microscopy images. Cell images obtained by flow imaging microscopy were analyzed with both the ParticleSentry^{AI} imaging software and a convolutional neural network (CNN) for fast and semi-automated viability assessment.

Throughout storage conditions similar to those during processing of CBMPs, a decrease in cell viability was observed over time for all conditions based on Annexin V and CalceinAM staining. Additionally, we observed a damaging effect of DMSO over time, whereas this effect was more pronounced at room temperature compared to refrigerated temperatures. The ParticleSentry^{AI} software was useful to detect qualitative differences in the cell viability as a shift towards non-viable cells could be observed throughout storage based on flow imaging microscopy images without prior sample preparation. Viability determination based on the CNN underestimated cell viability when compared to the flow cytometry assays, however the same trends were determined.

In summary, non-frozen storage of CBMPs should be kept to a minimum. However, standing times throughout the manufacturing of CBMPs as well as during in-use cannot be completely avoided and therefore, the optimal storage conditions have to be carefully evaluated. Additionally, further analytical development is needed to implement machine learning tools suitable for reliable viability quantification without additional sample preparation such as staining.

1. Introduction

Cell-based medicinal products (CBMPs) are a promising new class of biopharmaceuticals for the treatment of severe diseases such as cancer or genetic diseases [1]. Most commonly used cell types in clinical development are currently T cells, followed by stem cells and dendritic cells [2]. Also, six chimeric antigen receptor (CAR) T cells products are approved by the European Medicine Agency [3]. CAR T cells are genetically modified T cells to target cancer cells [4], whereas the CAR consists of an antigen-recognition domain fused to the T cell receptor [5]. The success of CBMPs depends on their effective manufacturing, which has an impact on product quality, patient safety and therapy effectiveness. CBMPs belong to the most complex biopharmaceutical products. They consist of living cells, which are either derived from the

* Corresponding author.
E-mail address: Tim.Menzen@coriolis-pharma.com (T. Menzen).

https://doi.org/10.1016/j.ejpb.2025.114703
Received 7 November 2024; Received in revised form 10 March 2025; Accepted 25 March 2025
Available online 26 March 2025

patient, i.e., autologous therapy, or are obtained from a donor, i.e., allogenic therapy [6]. The production process of CAR T cells is complex with several manufacturing steps from leukapheresis, transduction, expansion to fill-finish and distribution [1]. Fig. 1 shows a schematic overview of a CAR T cell production process from leukapheresis to the CAR T cell infusion. Within this process up to two cryopreservation processes may be applied, i.e., for the starting cell material after leukapheresis and for the final product [7]. Additionally, short-term liquid storage of the starting material is done up to 2–4 days at 2–8 °C [7,8].

Throughout each processing step cells may potentially be damaged leading to a decrease in cell viability and an increase in cell related impurities. Obtaining a high viability is critical to ensure a potent and safe drug product. Outside cell culture conditions the cell survival is limited to several hours to days depending upon the cell type and storage conditions [9,10]. Following CAR T cell production, the cells are usually cryopreserved with 5 to 10% dimethyl sulfoxide (DMSO) for frozen storage [7]. Although DMSO is a very effective cryoprotectant it has detrimental effects on cell viability at ambient temperatures [11]. Therefore, the exposure time of cells to DMSO must be kept to a minimum [11]. However, during the production process hold-times in cryoprotectant solution may occur, e.g., due to sample batch size and a prolonged filling procedure [12]. The effect of DMSO on cells can depend upon the used cell type, the storage condition (e.g., time and temperature), and the concentration of DMSO [11,13]. Additionally, the choice of the cell culture medium can influence the cell viability [14]. For T cells RPMI medium is commonly used for cell culture, however PBS is a standard solution for some handling steps such as washing for cell staining. Furthermore, some buffer systems are known to lead to changes in pH upon freezing such as phosphate buffers [15], which may influence the cell viability throughout cryopreservation. The implications of short-term liquid storage during CBMP processing on cell viability need to be explored further to define accurate limits for holding times.

To evaluate cell viability, fluorescence-based assays are most commonly used in combination with flow cytometry [16]. Additionally, machine learning tools are increasingly explored for the analysis of cells [17,18]. Previously, flow imaging microscopy (FIM) in combination with a convolutional neural network (CNN) was used to differentiate between viable and dead cells without any additional sample preparation such as staining [19]. Similarly, Thite and coworkers recently investigated the viability of Jurkat cells by using both a supervised (CNN) and unsupervised (variational autoencoder) machine learning approach [18].

The aim of this study was to evaluate cell stability, i.e., cell viability and membrane integrity, throughout liquid storage of cells in different media. Jurkat cells, an immortalized T cell line, were used as a model for CAR T cells [20,21]. Two novel AI tools trained on images derived from FIM for assessment of cell viability were applied. In the first approach a CNN was used as image classifier, i.e., the network is intended to process an image of an unknown particle and to assign that particle to one of the four training classes. Additionally, we used the software ParticleSentry^{AI}, which is generating the morphological "fingerprints" of the cells in a similar way as Thite et al. by combining a CNN with a dimensionality reduction to a 2D embedding of the feature vectors. Subsequently, all 2D embeddings of the cells are shown as probability density estimations, i.e., as "fingerprints" using a kernel density estimation [22]. This approach has been successfully applied to characterize differences in morphology of particles in pharmaceutical protein formulations [22,23].

Within the study, cell viability obtained from traditional flow cytometry with cell staining was compared to viability obtained from FIM by using either cell image classification as well as qualitative morphological "fingerprints".

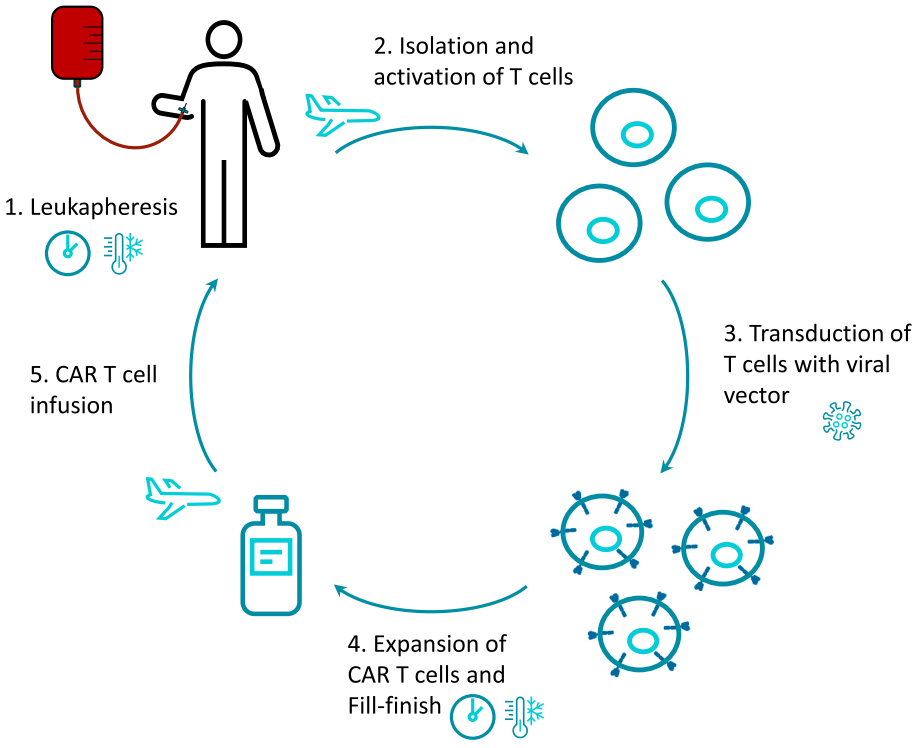

Fig. 1. Exemplary overview of the production process of CAR T cells. Leukapheresis is used to obtain the cellular starting material from the patient. Subsequently, T cells are isolated and activated by using immunomagnetic beads. Viral vectors are used for the transduction of the CAR. CAR positive T cells are expanded and the final drug product is prepared. Finally, CAR T cells are shipped to the treatment site and administered to the patient. During the production process cryopreservation (highlighted by thermostat) or hold times (highlighted by clock) can occur after leukapheresis and after fill-finish.

2. Material & methods

2.1. Cell material

Jurkat cells obtained from CLS GmbH (Eppelheim, Germany) were used within this study. Jurkat cell culture medium consisted of Roswell Park Memorial Institute (RPMI) 1640 medium (Gibco, ThermoFisher Scientific) with 10% fetal calf serum (Bio&Sell GmbH). Cell concentrations ranged between 0.5 and 3 x 10^6 cells/ml and Jurkat cells were freshly harvested by centrifugation at 400 g for 5 min followed by resuspension in the respective testing solution.

2.2. Stability of cells during short liquid storage

Cell stability, i.e., number of viable cells in comparison to apoptotic and necrotic cells as well as cell debris, was evaluated in different media throughout storage of cells.

The impact of medium on Jurkat cell viability was analyzed. Therefore, freshly harvested cells were centrifuged (400 g, 5 min) and resuspended in either RPMI 1640 or in PBS and subsequently stored in glass vials for 24 h at 25 °C and 60% relative humidity. The impact of medium was determined by analyzing the cells directly after harvest as well as after 24 h.

Similarly, the impact of different pH values on Jurkat cells was assessed, as pH shifts during freezing may occur, depending on the buffer system used [15]. Two different solutions were prepared by adjusting the pH of RPMI 1640 medium (pH 7.4) to pH 6.4 with hydrochloric acid or with sodium hydroxide to pH 8.4. Additionally, untreated RPMI 1640 was used as normal pH medium at pH 7.4. Freshly harvested cells were aliquoted, centrifuged (400 g, 5 min) and resuspended in the required pH solution. The solutions were aliquoted into glass vials and stored for 24 h at 25 °C and 60% relative humidity.

Additionally, the impact of DMSO on cell viability was determined. Therefore, Jurkat cells were centrifuged (400 g, 5 min) and resuspended in RPMI 1640 supplemented with 10 % DMSO. The cells were filled in glass vials and subsequently stored at 25 °C and 60% relative humidity or refrigerated at 2-8 °C for 24 h. The cells were analyzed after 3 h, 6 h and 24 h.

All measurement timepoints were analyzed with FIM to capture brightfield images as well as imaging flow cytometry (IFC) to measure viability based on fluorescence staining as described below.

2.3. Cell viability obtained from imaging flow cytometry (IFC)

An Amnis FlowSight imaging flow cytometer with a 488-nm fluorescence excitation laser was used to assess cell viability based on fluorescence staining. A combination of CalceinAM (Sigma Aldrich) and propidium iodide (Invitrogen, ThermoFisher Scientific) was used to stain viable and dead cells, respectively. Therefore, 200 µl of cells with 1x10^6 cells/ml were centrifuged (400 g, 5 min) and resuspended in PBS (Gibco™, ThermoFisher Scientific) prior addition of 0.5 µl of 2.5 µg/ml of CalceinAM and 2 µl of 100 µg/ml of PI. Cells were incubated in the dark for 20 min and subsequently analyzed via IFC.

Additionally, Annexin V staining was performed by using the Dead Cell Apoptosis Kit with Annexin V for flow cytometry with FITC and PI (Invitrogen, ThermoFisher Scientific) according to the manufacturer's instructions. In short, cells were washed with PBS followed by centrifugation and resuspension in 1x Annexin V binding buffer. To 100 µl of 1x10^6 cells/ml sample 5 µl of Annexin V-FITC and 1 µl of 100 µg/ml PI were added. The cells were incubated in the dark for 15 min prior IFC measurements.

CalceinAM and Annexin V staining was performed for samples stored at different pH and in different media. Jurkat cells stored in 10% DMSO solutions were only measured with Annexin V-staining and FIM. CalceinAM was not measured for the samples stored in DMSO for practical reasons as the samples were analyzed in short intervals after 3 h, 6 h and 12 h. Both assays CalceinAM and Annexin V require an incubation time of 20 min and 15 min, respectively. As duplicates were measured the measurement time for all three methods, i.e., Annexin V, CalceinAM and FIM would have been too long to adequately measure after 3 h and 6 h. Therefore, only Annexin V and FIM were measurable in parallel.

2.4. Cell viability obtained from flow imaging microscopy (FIM)

A FlowCam 8100 (Fluid Imaging Technologies) with a high-resolution CMOS camera (1920x1200 pixels) and a 20x magnification objective was used to image the cell samples. Intensity thresholds to detect particles were set to 12 for light and dark pixels and an imaging rate of 27 frames per seconds was used. Between measurement the instrument was cleaned with Terg-a-zyme enzyme detergent solution (1% [w/v]) and highly purified water.

2.5. Image generation for training of the supervised machine learning tools

For each class, i.e., viable, apoptotic, necrotic cells and cell debris, training images were generated by FIM. Jurkat cells were measured directly after harvest to obtain images for mostly viable cells. Furthermore, apoptosis was induced with Staurosporin (1 µM to 5x10^5 cells for 3 h) to generate a mostly apoptotic cell sample, which was measured with FIM. An apoptosis rate of 90–95% was confirmed by Annexin V-FITC staining and subsequent measurement via flow cytometry. Additionally, necrotic cells were generated by heat stress (55 °C for 90 min) as well as ethanol (10% (v/v) for 90 min) resulting in viabilities of 3.0% and 55.2%, respectively. Lastly, images of cell debris were measured for cell samples either vortexed for two minutes or after two freeze–thaw cycles (−140 °C to 37 °C). For all four classes training images were manually selected (4000–4500 images per class).

2.6. Qualitative cell viability obtained from cell image fingerprints

FIM images were analyzed using the commercial software ParticleSentry^{AI} (SentrySciences, version 2.3.1.0) to obtain the morphological "fingerprint" of the cell images. The "fingerprinting" approach is described in detail elsewhere [22]. In short, selected training images of cells for each class, i.e., viable, apoptotic, necrotic and cell debris, were used to train a CNN using a triplet loss approach. For each class above mentioned 4000 to 4500 images were used to train the CNN. The trained network was subsequently used to map the FIM images of testing data sets as individual 2D image embeddings or as a probability density function, i.e., sample fingerprint showing mode (max density value). Changes in the fingerprints of cell samples throughout storage were evaluated upon comparison to the trained model and observed visually.

2.7. Quantitative cell viability obtained from CNN classification

To quantify the loss in cell viability, the cell images obtained from FIM were classified as live (viable), apoptotic, or dead (necrotic or debris) cells by using a trained CNN model. A CNN was trained using a base EfficientNet B0 network pretrained on ImageNet [24] and then, with the first layer frozen, refined to predict between viable, apoptotic, necrotic, or debris classes as selected from the FIM images as mentioned above. Images were prepped for training by padding out to a consistent image size with pixels at zero. This technique permits initial image size to play a role in training. These images were normalized and flipped horizontally and vertically to increase sample size. Each experiment's images underwent the same pre-processing steps prior to prediction by the trained CNN. The trained CNN was used to predict the viability of stressed Jurkat cells.

2.8. Statistical analysis

Statistical analysis was performed by using Graphpad Prism 9.5. Results are reported as mean values ± standard deviation. One-way ANOVA followed by Tukey's test was performed to compare cells stored in different conditions. Results were considered significant, when $p < 0.05$.

3. Results

3.1. Implementation of image analysis based on machine learning tools

Two different machine learning approaches were used to evaluate changes in cell viability qualitatively and quantitatively based on FIM images. An overview of the established tools can be seen in Fig. 2. Four different cell classes were differentiated, i.e., viable, apoptotic or necrotic cells and cell debris. For each class except viable training images were generated by treatment of the cells to enrich for debris and apoptotic and necrotic cells and subsequent manual selection in these treated cell populations (Fig. 2A). Images of viable cells for training were obtained by manual selection of cells measured directly after cell harvest. These images were (i) used to train a CNN for image classification (Fig. 2B and D) as well as (ii) analyzed with the ParticleSentry^{AI} software to generate a fingerprint for each sample (Fig. 2C and E). In ParticleSentry^{AI} the CNN is trained to create a two-dimensional representation of each image. The fingerprint is the probability density estimate of the lower dimensional 2D representation of a collection of images (Fig. 2C and E). The confusion matrix for the CNN shows good classification for all four classes with around 0.84 to 0.89 correctly classified images (Fig. 2B). Subsequently, the CNN was used to determine the viability of cells stored under different conditions, e.g., upon storage in PBS in comparison to RPMI (Fig. 2D). The ParticleSentry^{AI}

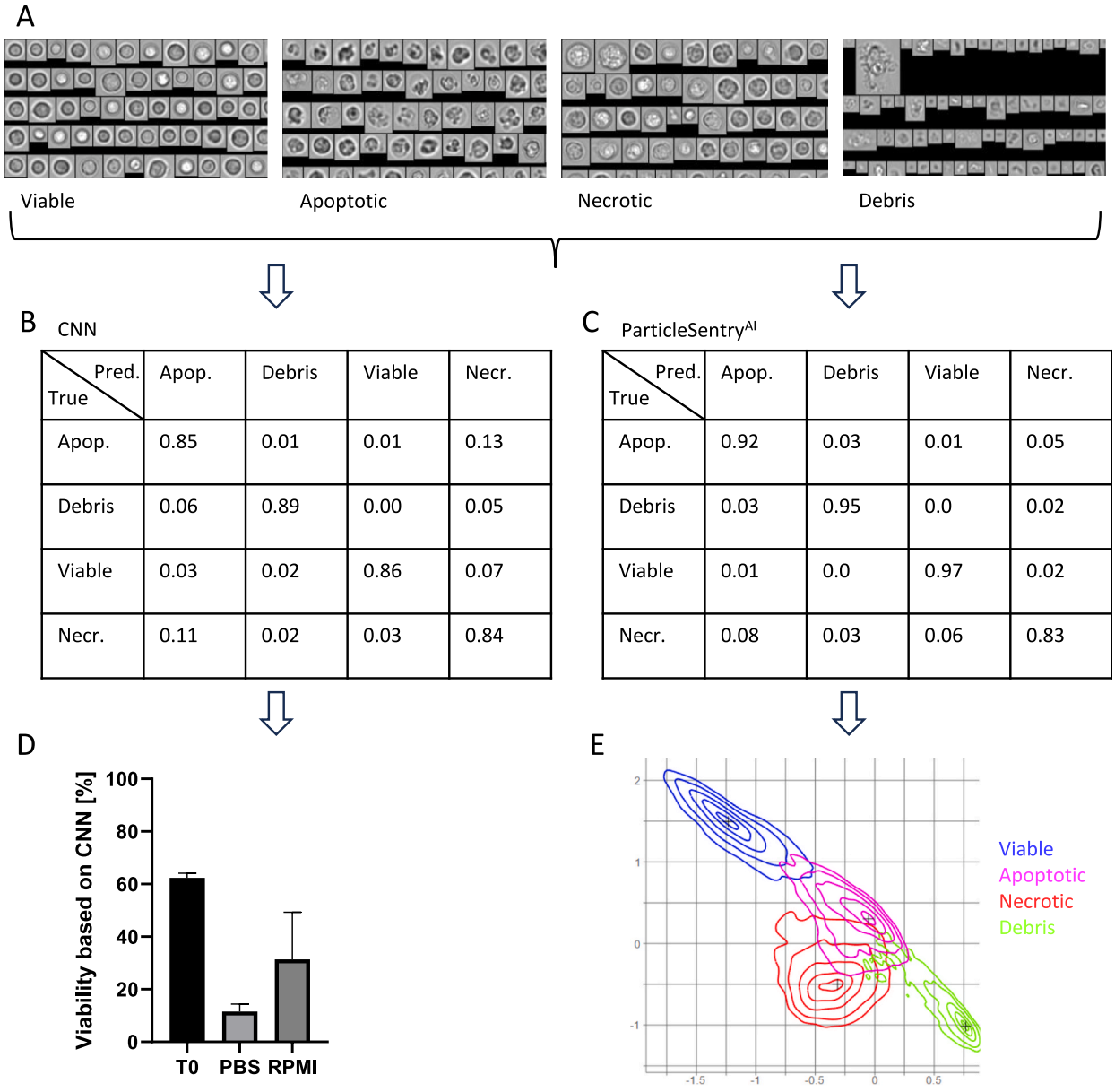

B CNN

True \ Pred.	Apop.	Debris	Viable	Necr.
Apop.	0.85	0.01	0.01	0.13
Debris	0.06	0.89	0.00	0.05
Viable	0.03	0.02	0.86	0.07
Necr.	0.11	0.02	0.03	0.84

C ParticleSentry^{AI}

True \ Pred.	Apop.	Debris	Viable	Necr.
Apop.	0.92	0.03	0.01	0.05
Debris	0.03	0.95	0.0	0.02
Viable	0.01	0.0	0.97	0.02
Necr.	0.08	0.03	0.06	0.83

Fig. 2. Exemplary images of the manually curated set of training images (A). Training images were used to train a model within ParticleSentry^{AI} as well as a CNN. Confusion matrices for both models are shown (B: CNN; C: ParticleSentry^{AI}), whereas rows represent the actual class (true) and columns the predicted class (pred.). The CNN was used to determine cell viability of cells stored at different conditions (D). The established ParticleSentry model was used to generate a fingerprint (E), which shows the 2D embeddings of all four classes in an estimated probability density. The fingerprints were used to evaluate qualitative viability changes throughout cell storage.

CNN showed a slightly better classification rate with 0.92 to 0.97, except for necrotic cells with 0.83 (Fig. 2C). The resulting fingerprint of the images shows a good differentiation between viable and non-viable cells, whereas apoptotic and necrotic images overlap (Fig. 2E).

3.2. Stability of cells during short liquid storage outside cell culture conditions

To evaluate the impact of storage conditions on cell viability outside cell culture conditions, Jurkat cells were stored in different conditions over a period of up to 24 h hours and subsequently analyzed via IFC and FIM. In general, a decrease in cell viability was observed over time for all samples including control in RPMI medium. Fig. 3 shows a viability comparison of Jurkat cells stored at 25 °C and 60% relative humidity (RT) as measured with CalceinAM and Annexin V staining as well as CNN analysis and changes in the fingerprint of the FIM images. A decrease in viability was determined based on fluorescence measurements with CalceinAM and Annexin V staining (Fig. 3A and B). For both assays an approximately 20% lower viability was observed for the cells stored PBS in comparison to RPMI. Additionally, Annexin V viabilities were around 20% lower than the values obtained for CalceinAM. The CNN is generally underestimating the cell viability with 62% viable cells for T0 in comparison to 90% (CalceinAM) and 87% (Annexin V). The overall viability trend measured based on CNN is similar to the fluorescence assays with PBS resulting in lower viabilities than RPMI (Fig. 3C). At T0 most cells are located in the viable region of the fingerprint as well as in the debris region (compared to Fig. 2D), whereas after 24 h the fingerprint slightly shifts towards apoptotic and necrotic cells for cells stored in RPMI medium. The fingerprint of Jurkat cells stored in PBS shifts completely towards apoptotic, necrotic and debris cells.

Furthermore, the impact of different pH values on cell viability was determined for cells stored at room temperature over 24 h in RPMI at pH 6.4, pH 7.4 and pH 8.4 (Fig. 4). A decrease in viability was observed during storage based on fluorescence measurements, although CalceinAM based viabilities were slightly higher in comparison to Annexin V measured values. For CalceinAM no difference can be observed for cells stored at pH 6.4 and pH 7.4 with viabilities of 90.6% ± 0.5% and 89.0% ± 1.0%, respectively. A minor decrease was observed at pH 8.4 (79.7% ± 2.7%). However, the differences upon storage are more pronounced when using Annexin V to measure viability with the decreasing viability from pH 6.4 (76.8% ± 5.0%) over pH 7.4 (55.7% ± 3.7%) to pH 8.4 (46.2% ± 2.5%). The viability values based on the CNN are lower (between 36% and 67 %), whereas the overall trend is the same in comparison to the fluorescence staining. Similar to cells stored in different media a shift of the ParticleSentry^{AI} fingerprint can be observed after 24 h of storage towards non-viable cells, especially necrotic cells and cell debris (Fig. 4D). This shift is slightly more pronounced for cells stored at pH 7.4 and pH 8.4.

Lastly, the impact of 10% DMSO on the viability of Jurkat cells was evaluated based on ParticleSentry^{AI}, Annexin V staining and CNN. Therefore, the cells were stored in either RPMI alone or in RPMI with 10% DMSO at room temperature as well as refrigerated (2-8 °C). Fig. 5 shows the impact of DMSO on Jurkat cells throughout storage for up to 24 h at room temperature and Fig. 6 shows the impact at 2–8 °C. For cells stored at both temperatures a decrease in cell viability over time was observed for both RPMI only and RPMI with 10% DMSO, whereas the damaging effects at 2-8 °C seem to be reduced. Jurkat cells in RPMI dropped to 42.7 % ± 5.9 % viability at room temperature, but only to 61.8% ± 0.3% at 2-8 °C after 24 h based on Annexin V. Also, the damaging effect of DMSO was slightly reduced for cells stored refrigerated (23.3% ± 2.2%) compared to RT (7.9% ± 0.2%) based on Annexin V. A damaging effect of DMSO was already visible after short-term storage of 3 h at RT (Annexin V). Based on CNN no clear effect of DMSO over time could be observed with a drop in viability for DMSO only after 24 h. A clear shift towards non-viable cells and cell debris can be seen in the fingerprints for cells stored at room temperature after 24 h, whereas this effect is more pronounced in the cells stored in RPMI with 10% DMSO. The damaging effect of liquid storage can also be observed after 24 h in the fingerprints for the cells stored at 2-8 °C,

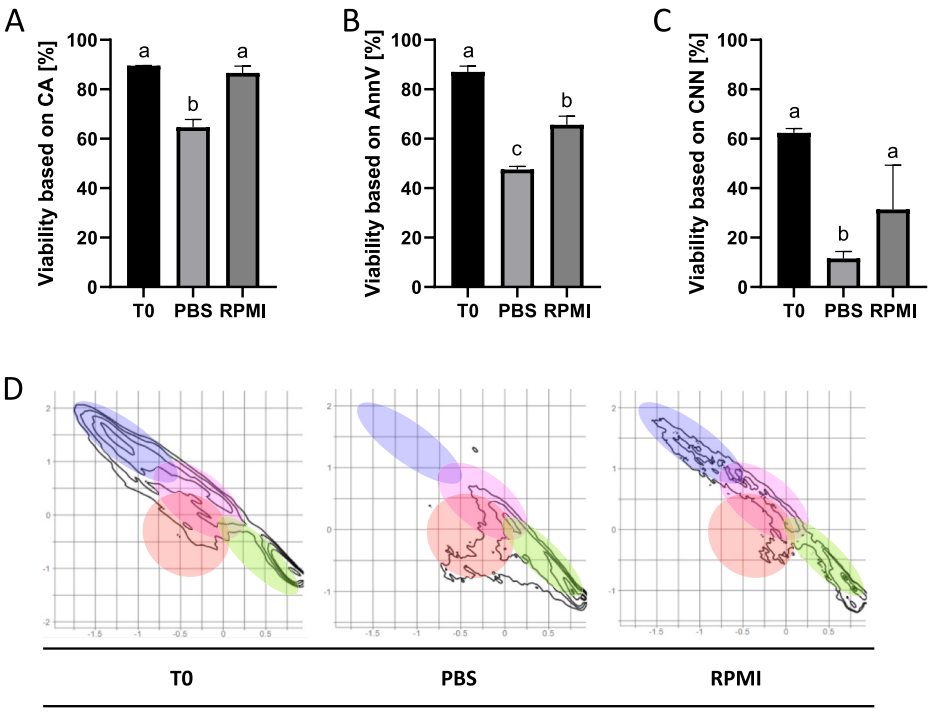

Fig. 3. Impact of the used medium on Jurkat cell viability stored for 24 h at room temperature as measured using IFC analysis with CalceinAM (A), Annexin V (B), CNN (C) and with ParticleSentry^{AI} (D). Colored regions highlight the approximate location of cell classes of the fingerprint models (blue: viable cell; pink: apoptotic cells; red: necrotic cells; green: cell debris). Statistically significant differences ($p \leq 0.5$) based on one-way ANOVA followed by Tukey's test are indicated by different letters. (For interpretation of the references to colour in this figure legend, the reader is referred to the web version of this article.)

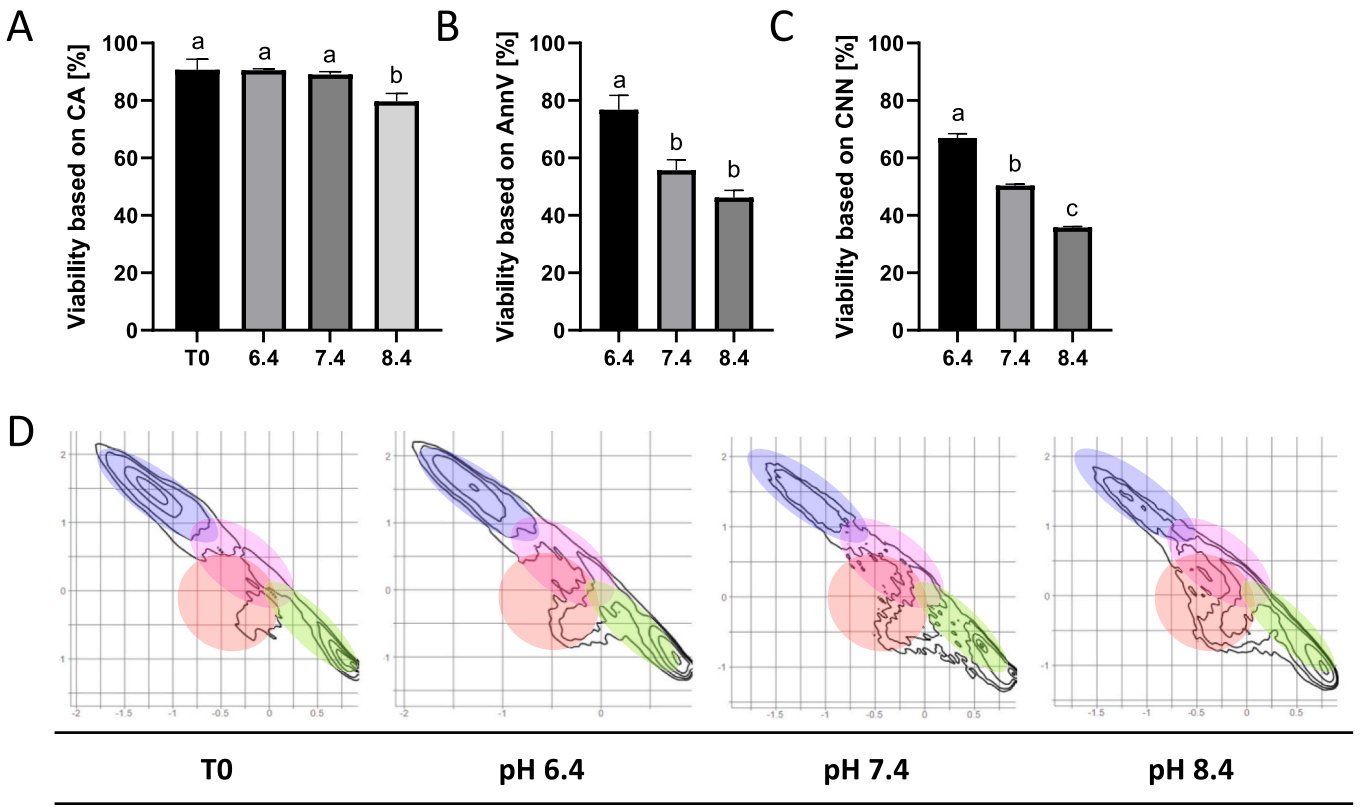

Fig. 4. Impact of the pH value on cell viability as measured with CalceinAM (A), Annexin V (B), CNN (C) and ParticleSentry^{AI} (D) for Jurkat cells stored for 24 h at room temperature. RPMI at pH 6.4 (A), pH 7.4 (N) and pH 8.4 (B). Colored regions highlight the approximate location of cell classes of the fingerprint models (blue: viable cell; pink: apoptotic cells; red: necrotic cells; green: cell debris). Statistically significant differences ($p \leq 0.5$) based on one-way ANOVA followed by Tukey's test are indicated by different letters. (For interpretation of the references to colour in this figure legend, the reader is referred to the web version of this article.)

although to a lesser extent.

4. Discussion

To produce efficacious CBMPs of high product quality it is critical to ensure a high cell viability and low impurities such as dead and apoptotic cells and other debris particles. Therefore, it is important to (i) characterize the composition of cells and particular impurities in the CBMP and (ii) understand different impact factors on cell viability throughout manufacturing and in-use of the CBMP such as hold times outside cell culture conditions and medium composition (formulation). In this study the viability of Jurkat cells was determined based on analysis of FIM images by ParticleSentry^{AI} software (qualitatively) as well as a CNN (quantitatively) without any sample preparation such as staining as well as imaging flow cytometry by using two fluorescent stains.

Regarding the stability of Jurkat cells, several observations were made. In general, longer standing times of cells should be avoided as cells outside cell culture conditions will show a decrease in cell viability. It has been previously shown that prolonged storage of peripheral blood stem cells (PBSC) at 4 °C for up to 4 days did lead to a reduced cell recovery and cell viability after storage [10]. Additionally, the choice of intermediate storage solutions should be selected with care and long hold times should be avoided as storage in PBS led to a lower cell viability in comparison to storage in RPMI within this study. Decrease of cell viability upon prolonged storage in PBS was previously reported in the literature for different cell types [25,26]. For instance, storage of Chinese hamster ovary cells in PBS for 1 h prior viability measurements did already result in a reduced viability compared to cells measured directly after dilution in PBS [25], highlighting the need to limit the standing time of cells in PBS. Furthermore, the impact of pH upon cell viability was determined. In general, fluctuations of the pH should be avoided as cells are sensitive towards the environmental pH [27,28]. Cells are usually cultured in buffered solutions using a CO_2-bicarbonate system, which requires a 5% CO_2 atmosphere [29]. Additionally, non-volatile buffers such as HEPES, PIPES or MES can be used, which maintain the pH independent of the atmospheric CO_2 level and are advantageous when handling cells outside a cell incubator [29]. The buffer system also comes into play upon freezing of cells. Due to the limited shelf-life of liquid CBMPs, CBMPs are usually stored cryopreserved. Depending upon the used buffer system changes in the pH can occur upon freezing with sodium phosphate buffer resulting in the highest pH change compared to acetate or citrate [15].

Furthermore, the impact of DMSO on the viability of Jurkat cells was evaluated during intermediate storage at room temperature or 2-8 °C. A decrease in viability for cells stored in DMSO was observed during storage at room temperature with ParticleSentry^{AI} and with Annexin V staining but not with the CNN. Storage at 2-8 °C minimized the DMSO stress. A lower cytotoxicity of DMSO upon storage at refrigerated temperatures has previously been reported for different cell types [30,31]. The detrimental effect of DMSO after intermediate storage prior cryopreservation has been shown before for cord blood mononuclear cells, when incubation times exceeded 1 h [11]. Numerous studies have demonstrated the negative impact of DMSO on cell proliferation of T cells [13,32,33] and proinflammatory cytokine production such as interleukin-2 and interferon-γ [32–34]. One possible mechanism of toxicity of DMSO is related to its impact on cell membranes, which is membrane thinning, induction of water pores or disintegration of the bilayer structure depending upon the DMSO concentration [35]. The damaging effect of DMSO is temperature-dependent and destabilization of cell membranes is increased at higher temperatures [36].

Also, viability values for cells stored in RPMI without DMSO at 2-8 °C

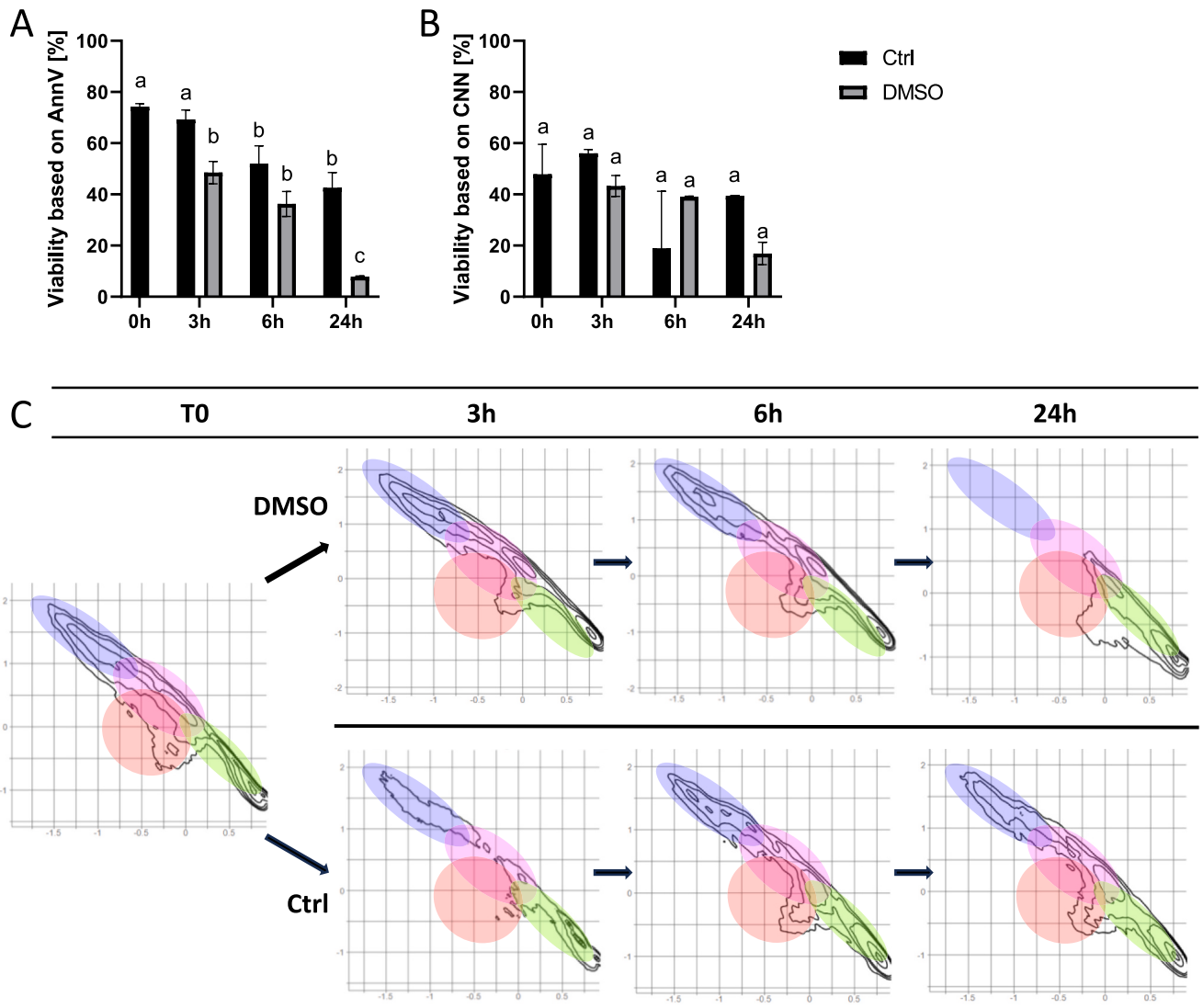

Fig. 5. Impact of DMSO on cell viability as measured with Annexin V (A), CNN (B) and ParticleSentry^{AI} (C) for Jurkat cells stored at room temperature. Cells were measured as duplicate measurements after 3 h, 6 h and 24 h of storage in RPMI (Ctrl) or 10% DMSO in RPMI (DMSO). Colored regions highlight the approximate location of cell classes of the fingerprint models: blue: viable cell; pink: apoptotic cells; red: necrotic cells; green: cell debris (C). Statistically significant differences ($p \leq 0.5$) based on one-way ANOVA followed by Tukey's test are indicated by different letters. (For interpretation of the references to colour in this figure legend, the reader is referred to the web version of this article.)

were higher than for storage at room temperature within this study, indicating the potential benefit of refrigerated temperature for short-term Jurkat cell storage. A similar temperature effect was previously reported for leukapheresis starting materiel, which showed higher viability for storage at 2-8 °C in comparison to 10-25 °C [37]. Additionally, it was shown that for hematopoietic progenitor cells intermediate storage in a refrigerator led to higher cell recoveries than for cells stored at room temperature [38]. Also, refrigerated overnight storage of peripheral blood stem cells led to a higher cell recovery compared to overnight storage at room temperature [39]. On the other hand, prolonged storage of blood at refrigerated temperature did have a negative impact on the subsequent isolation of peripheral mononuclear blood cells and room temperature storage is recommended [40], highlighting the need to analyze the appropriate (intermediate) storage conditions for each cell type and application.

In general, the liquid storage of cells should be avoided especially for prolonged periods. However, if immediate processing of cells is not feasible the storage conditions such as medium and temperature should be evaluated carefully for each cell type. Within this study storage in RPMI as well as refrigerated temperatures were identified as optimal conditions for short-term liquid storage of Jurkat cells outside cell culture conditions. Storage of Jurkat cells in RPMI should be less than 3 h, when stored at room temperature and less than 6 h, when stored at 2-8 °C. Due to the toxicity of DMSO storage in DMSO should generally be avoided and contact time in liquid solution should be kept to a minimum. However, if intermediate storage is unavoidable due to the fill-finish process of CBMPs, storage in DMSO should be at 2-8 °C and limited to a maximum of 3 h considering that shorter storage results in less cell damage. Storage conditions for primary human T cells may differ, possibly also depending on the donor. However, limits and storage conditions for Jurkat cells can be used as a guidance, when evaluating T cells.

To determine cell viability different methods based either on fluorescence staining or machine learning tools were applied. In summary, the same trends were determined with regard to the effect of storage formulation and temperature on cell viability based on the ParticleSentry^{AI} software as well as the CNN. Based on the ParticleSentry^{AI} software qualitative differences in the cell viability of Jurkat cells could be observed during 24 h storage in different media. However, viability determination based on CNN resulted in lower cell viability compared to

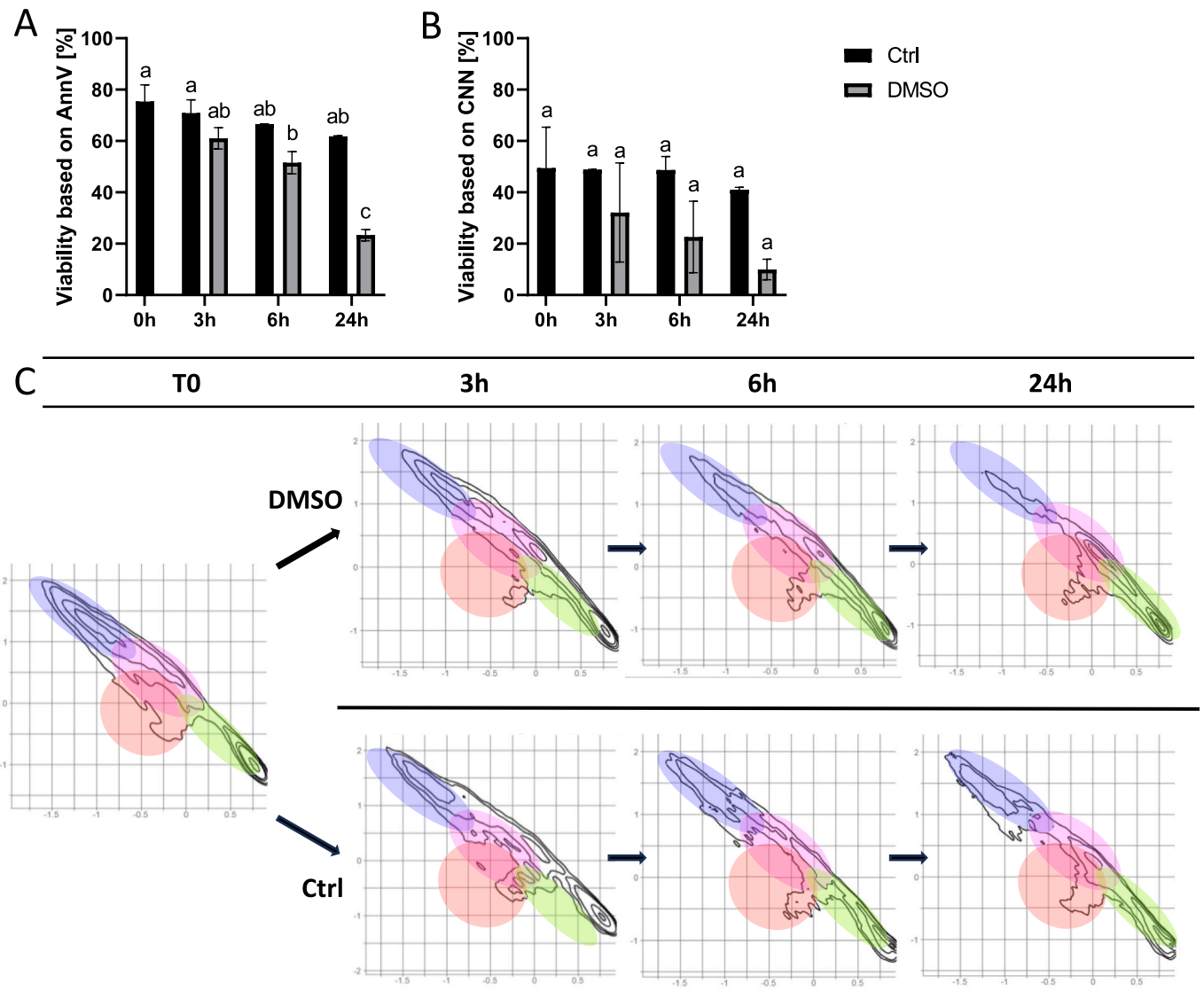

Fig. 6. Impact of DMSO on cell viability as measured with Annexin V (A), CNN (B) and ParticleSentry^{AI} (C) for Jurkat cells stored at 2–8 °C. Cells were measured as duplicate measurements after 3 h, 6 h and 24 h of storage in RPMI (Ctrl) or 10% DMSO in RPMI (DMSO). Colored regions highlight the approximate location of cell classes of the fingerprint models: blue: viable cell; pink: apoptotic cells; red: necrotic cells; green: cell debris (C). Statistically significant differences ($p \leq 0.5$) based on one-way ANOVA followed by Tukey's test are indicated by different letters. (For interpretation of the references to colour in this figure legend, the reader is referred to the web version of this article.)

the biochemical assays routinely used. Depending upon the used storage condition the viability prediction deviated more or less from the values obtained by fluorescence staining. For instance, storage of the cells in PBS for 24 h led to very low viability values by CNN (11% ± 3%) in comparison to fluorescence staining with Annexin V (47% ± 1%), whereas the DMSO experiments showed a slightly better correlation between the methods, e.g., after 24 h at room temperature with 39% ± 0% (CNN) and 43% ± 6% (Annexin V). As CNNs are highly specific models the selection of the training images can influence their prediction capabilities. In this study, training images for apoptotic cells were generated by using staurosporin, whereas necrotic images were generated with ethanol or by applying heat. Viable training cell images were measured with freshly harvested cells. However, the testing samples were stored for up to 24 h outside cell culture conditions in different cell media. Based on fluorescence-based assays a cell can be measured as viable if its membrane is still intact (CalceinAM) or apoptosis markers are absent (Annexin V), although the cell morphology might have changed leading to a non-viable classification based on the CNN. We acknowledge that there is deviation between the CNN predicted value and the results of flow cytometry. While we did attempt to optimize the CNN model by providing different training image sets for each of the conditions (data not shown), further optimization of the CNN could possibly be achieved by including additional training images of cells under different storage conditions, e.g., after storage at room temperature or after storage in DMSO. Additionally, image size did possibly have an impact on the CNN's viability prediction. Images were prepared for training and testing with the CNN by padding to the same image size. Within this study two different padding approaches were initially tested, i.e., padding with 0 and padding with the average pixel. A comparison for both padding approaches can be found in the appendix (Fig. S1). A better correlation with fluorescence-based viability values were obtained for the padding with 0 approach and therefore used throughout this study. We trained a series of AIs with varying model hyperparameters, such as number of layers and learning rate. However, further investigation into varying these parameters, in particular image size, could help improve the predictability of the CNN [41].

In general, the development of novel approaches to determine cell viability based on stain-free image analysis by using machine learning

tools would improve CBMPs quality assessment. Currently used fluorescence assays require (multiple) dyes and several preparation steps including cell washing and incubation times are needed [19]. Preparation steps can have a detrimental effect on cell viability, e.g., washing and resuspension of cells in PBS can lead to cell damages due to osmotic stress or cell loss [42–44]. On the other hand, stain-free approaches allow for minimal cell manipulation reducing the risk of cell damages throughout sample preparation. However, fluorescence staining remains to be the gold-standard for cell viability determination and machine learning based approaches need to be further optimized.

5. Conclusion

In this study the stability of cells during short-term liquid storage was evaluated as standing times of cells can occur during processing of CBMPs. In general, liquid storage of cells outside of cell culture conditions should be avoided and limited to 3 h as cell viability will decrease quite quickly. Additionally, storage in saline solutions such as PBS is not recommended and RPMI is the preferred intermediate storage solution. Furthermore, prolonged exposure to DMSO should be avoided as it has a detrimental effect on cell viability. This effect can be slightly reduced by storing the cells at 2-8°C. Novel machine learning tools can complement standard flow cytometric analysis of cells. FIM with image analysis based on machine learning can be used to qualitatively and quantitatively determine cell viability without complex sample handling. In general, CNN and fluorescence staining showed the same trend, but viability values highly varied between the methods. Although different methods will not necessarily result in the same outcomes as they are based on different measurement principles, more investigation is required to understand the observed differences. As cell samples are never alike and cell quality can fluctuate depending upon the time of harvest, analytical development is challenging. Therefore, more research is necessary to improve the analytical characterization as well as our understanding on stability of CBMPs.

CRediT authorship contribution statement

Alexandra Roesch: Writing – original draft, Visualization, Investigation, Data curation, Conceptualization. **Cornelia Hiemenz:** Investigation. **Teresa Findley:** Software, Investigation, Conceptualization. **Ilya Goldberg:** Software, Conceptualization. **Roland Windisch:** Resources, Investigation. **Christian Wichmann:** Resources. **Gideon Kersten:** Writing – review & editing, Supervision, Conceptualization. **Tim Menzen:** Writing – review & editing, Supervision, Conceptualization.

Appendix A. Supplementary material

Supplementary data to this article can be found online at https://doi.org/10.1016/j.ejpb.2025.114703.

Data availability

Data will be made available on request.

References

[1] A. Bak, K.P. Friis, Y. Wu, R.J.Y. Ho, Translating cell and gene biopharmaceutical products for health and market impact. Product scaling from clinical to marketplace: lessons learned and future outlook, J. Pharm. Sci. 108 (2019) 3169–3175, https://doi.org/10.1016/j.xphs.2019.05.027.

[2] L.-L.-W. Wang, M.E. Janes, N. Kumbhojkar, N. Kapate, J.R. Clegg, S. Prakash, M. K. Heavey, Z. Zhao, A.C. Anselmo, S. Mitragotri, Cell therapies in the clinic, Bioeng. Transl. Med. 6 (2021) e10214, https://doi.org/10.1002/btm2.10214.

[3] S. Bellino, A. La Salvia, M.F. Cometa, R. Botta, Cell-based medicinal products approved in the European Union: current evidence and perspectives, Front. Pharmacol. 14 (2023) 1200808, https://doi.org/10.3389/fphar.2023.1200808.

[4] M.-R. Benmebarek, C.H. Karches, B.L. Cadilha, S. Lesch, S. Endres, S. Kobold, Killing mechanisms of chimeric antigen receptor (CAR) T cells, Int. J. Mol. Sci. 20 (2019), https://doi.org/10.3390/ijms20061283.

[5] V. Picanço-Castro, K. Swiech, K.C.R. Malmegrim, D.T. Covas, CAR-T Cells for Cancer Treatment: Current Design and Next Frontiers, in: K. Swiech, K.C. R. Malmegrim, V. Picanço-Castro (Eds.), Chimeric Antigen Receptor T Cells, Springer, US, New York, NY, 2020, pp. 1–10.

[6] K.H. Hoogendoorn, D.J.A. Crommelin, W. Jiskoot, Formulation of cell-based medicinal products: a question of life or death? J. Pharm. Sci. 110 (2021) 1885–1894, https://doi.org/10.1016/j.xphs.2020.07.002.

[7] M. Jandová, G.N. Stacey, M. Lánská, J. Gregor, P. Rozsívalová, L. Beková, Z. Woidigová Ducháová, D. Belada, J. Radocha, P. Měřička, B. Fuller, Perspective: the role of cryopreservation techniques in manufacturing, transport, and storage of car-T therapy products, Cryo Lett. 44 (2023) 123–133, https://doi.org/10.54680/fr23310110112.

[8] C. Correia, A. Koshkin, M. Carido, N. Espinha, T. Šarić, P.A. Lima, M. Serra, P. M. Alves, Effective hypothermic storage of human pluripotent stem cell-derived cardiomyocytes compatible with global distribution of cells for clinical applications and toxicology testing, Stem Cells Transl. Med. 5 (2016) 658–669, https://doi.org/10.5966/sctm.2015-0238.

[9] G.S. Kao, H.T. Kim, H. Daley, J. Ritz, S.R. Burger, L. Kelley, C. Vierra-Green, S. Flesch, S. Spellman, J. Miller, D. Confer, Validation of short-term handling and storage conditions for marrow and peripheral blood stem cell products, Transfusion 51 (2011) 137–147, https://doi.org/10.1111/j.1537-2995.2010.02758.x.

[10] A.B. Araújo, G.D. Salton, M.H. Angeli, J.M. Furlan, T. Schmalfuss, L.M. Röhsig, Effects of cell concentration, time of fresh storage, and cryopreservation on peripheral blood stem cells: PBSC fresh storage and cryopreservation, Transfus. Apher. Sci. 61 (2022) 103298, https://doi.org/10.1016/j.transci.2021.103298.

[11] L.J. Fry, S. Querol, S.G. Gomez, S. McArdle, R. Rees, J.A. Madrigal, Assessing the toxic effects of DMSO on cord blood to determine exposure time limits and the optimum concentration for cryopreservation, Vox Sang. 109 (2015) 181–190, https://doi.org/10.1111/vox.12267.

[12] J. Meneghel, P. Kilbride, G.J. Morris, Cryopreservation as a key element in the successful delivery of cell-based therapies-a review, Front. Med. 7 (2020) 592242, https://doi.org/10.3389/fmed.2020.592242.

[13] H. Kloverpris, A. Fomsgaard, A. Handley, J. Ackland, M. Sullivan, P. Goulder, Dimethyl sulfoxide (DMSO) exposure to human peripheral blood mononuclear cells (PBMCs) abolish T cell responses only in high concentrations and following coincubation for more than two hours, J. Immunol. Methods 356 (2010) 70–78, https://doi.org/10.1016/j.jim.2010.01.014.

[14] M. GŁaczynska, M. Machcinska, K. Donskow-Lysoniewska, Effects of different media on human T regulatory cells phenotype, In Vivo (Athens) 35 (2021) 283–289, https://doi.org/10.21873/invivo.12257.

[15] P. Kolhe, E. Amend, S.K. Singh, Impact of freezing on pH of buffered solutions and consequences for monoclonal antibody aggregation, Biotechnol. Prog. 26 (2010) 727–733, https://doi.org/10.1002/btpr.377.

[16] FDA/CBER, Considerations for the Development of Chimeric Antigen Receptor T Cell Products; Guidance for Industry (2024).

[17] T. Falk, D. Mai, R. Bensch, Ö. Çiçek, A. Abdulkadir, Y. Marrakchi, A. Böhm, J. Deubner, Z. Jäckel, K. Seiwald, A. Dovzhenko, O. Tietz, C. Dal Bosco, S. Walsh, D. Saltukoglu, T.L. Tay, M. Prinz, K. Palme, M. Simons, I. Diester, T. Brox, O. Ronneberger, U-Net: deep learning for cell counting, detection, and morphometry, Nat. Methods 16 (2019) 67–70, https://doi.org/10.1038/s41592-018-0261-2.

[18] N.G. Thite, E. Tuberty-Vaughan, P. Wilcox, N. Wallace, C.P. Calderon, T. W. Randolph, Stain-free approach to determine and monitor cell heath using supervised and unsupervised image-based deep learning, J. Pharm. Sci. (2024), https://doi.org/10.1016/j.xphs.2024.05.001.

[19] A.D. Grabarek, W. Jiskoot, A. Hawe, K. Pike-Overzet, T. Menzen, Forced degradation of cell-based medicinal products guided by flow imaging microscopy: explorative studies with Jurkat cells, Eur. J. Pharm. Biopharm. 167 (2021) 38–47, https://doi.org/10.1016/j.ejpb.2021.07.004.

[20] C. Carrasco-Padilla, O. Aguilar-Sopeña, A. Gómez-Morón, S. Alegre-Gómez, F. Sánchez-Madrid, N.B. Martín-Cófreces, P. Roda-Navarro, T cell activation and effector function in the human Jurkat T cell model, Methods Cell Biol. 178 (2023) 25–41, https://doi.org/10.1016/bs.mcb.2022.09.012.

[21] F. Jahan, J. Koski, D. Schenkwein, S. Ylä-Herttuala, H. Göös, S. Huuskonen, M. Varjosalo, P. Maliniemi, J. Leitner, P. Steinberger, H.-J. Bühring, K. Vettenranta, M. Korhonen, Using the Jurkat reporter T cell line for evaluating the functionality of novel chimeric antigen receptors, Front. Mol. Med. 3 (2023) 1070384, https://doi.org/10.3389/fmmed.2023.1070384.

[22] A.L. Daniels, C.P. Calderon, T.W. Randolph, Machine learning and statistical analyses for extracting and characterizing “fingerprints” of antibody aggregation at container interfaces from flow microscopy images, Biotechnol. Bioeng. (2020), https://doi.org/10.1002/bit.27501.

[23] A.E. Witeof, A.L. Daniels, L.T. Rea, S. Movafaghi, K. Kurtz, M. Davis, R.W. Eveland, C.P. Calderon, T.W. Randolph, Machine learning and accelerated stress approaches to differentiate potential causes of aggregation in polyclonal antibody formulations during shipping, J. Pharm. Sci. 110 (2021) 2743–2752, https://doi.org/10.1016/j.xphs.2021.02.029.

[24] O. Russakovsky, J. Deng, H. Su, J. Krause, S. Satheesh, S. Ma, Z. Huang, A. Karpathy, A. Khosla, M. Bernstein, A.C. Berg, L. Fei-Fei, ImageNet large scale visual recognition challenge, Int. J. Comput. Vis. 115 (2015) 211–252, https://doi.org/10.1007/s11263-015-0816-y.

[25] A. Chen, M. Leith, R. Tu, G. Tahim, A. Sudra, S. Bhargava, Effects of diluents on cell culture viability measured by automated cell counter, PLoS One 12 (2017) e0173375, https://doi.org/10.1371/journal.pone.0173375.

[26] N.-H. Yu, S.Y. Chun, Y.-S. Ha, H.T. Kim, D.H. Kim, J. Kim, J.-W. Chung, J.N. Lee, P. H. Song, E.S. Yoo, B.S. Kim, T.G. Kwon, Optimal stem cell transporting conditions

to maintain cell viability and characteristics, Tissue Eng. Regener. Med. 15 (2018) 639–647, https://doi.org/10.1007/s13770-018-0133-y.
[27] A.C. Taylor, Responses of cells to pH changes in the medium, J. Cell Biol. 15 (1962) 201–209, https://doi.org/10.1083/jcb.15.2.201.
[28] H. Eagle, The effect of environmental pH on the growth of normal and malignant cells, J. Cell. Physiol. 82 (1973) 1–8, https://doi.org/10.1002/jcp.1040820102.
[29] J. Michl, K.C. Park, P. Swietach, Evidence-based guidelines for controlling pH in mammalian live-cell culture systems, Commun. Biol. 2 (2019) 1–12, https://doi.org/10.1038/s42003-019-0393-7.
[30] S.H. Hristova, A.M. Zhivkov, Cytotoxicity of dimethyl sulfoxide on human hematopoietic stem cells at different temperatures, J. Appl. Hematol. 14 (2023) 263–267, https://doi.org/10.4103/joah.joah_96_23.
[31] A. Lawson, H. Ahmad, A. Sambanis, Cytotoxicity effects of cryoprotectants as single-component and cocktail vitrification solutions, Cryobiology 62 (2011) 115–122, https://doi.org/10.1016/j.cryobiol.2011.01.012.
[32] L. Abreu Costa, M. Henrique Fernandes Ottoni, M.G. Santos, A.B. Meireles, V. Gomes Almeida, W. Fátima Pereira, B. Alves Avelar-Freitas, G. Eustáquio Alvim Brito-Melo, Dimethyl sulfoxide (DMSO) decreases cell proliferation and TNF-α, IFN-γ, and IL-2 cytokines production in cultures of peripheral blood lymphocytes, Molecules (Basel, Switzerland) 22 (11) (2017) 1789, https://doi.org/10.3390/molecules22111789.
[33] L. Holthaus, D. Lamp, A. Gavrisan, V. Sharma, A.-G. Ziegler, M. Jastroch, E. Bonifacio, CD4+ T cell activation, function, and metabolism are inhibited by low concentrations of DMSO, J. Immunol. Methods 463 (2018) 54–60, https://doi.org/10.1016/j.jim.2018.09.004.
[34] M. Timm, L. Saaby, L. Moesby, E.W. Hansen, Considerations regarding use of solvents in in vitro cell based assays, Cytotechnology 65 (2013) 887–894, https://doi.org/10.1007/s10616-012-9530-6.
[35] A.A. Gurtovenko, J. Anwar, Modulating the structure and properties of cell membranes: the molecular mechanism of action of dimethyl sulfoxide, J. Phys. Chem. B 111 (2007) 10453–10460, https://doi.org/10.1021/jp073113e.
[36] T.J. Anchordoguy, J.F. Carpenter, J.H. Crowe, L.M. Crowe, Temperature-dependent perturbation of phospholipid bilayers by dimethylsulfoxide, BBA 1104 (1992) 117–122, https://doi.org/10.1016/0005-2736(92)90139-D.
[37] S. Tyagarajan, D. Schmitt, C. Acker, E. Rutjens, Autologous cryopreserved leukapheresis cellular material for chimeric antigen receptor-T cell manufacture, Cytotherapy 21 (2019) 1198–1205, https://doi.org/10.1016/j.jcyt.2019.10.005.
[38] L.J. Fry, S.Q. Giner, S.G. Gomez, M. Green, S. Anderson, J. Horder, S. McArdle, R. Rees, J.A. Madrigal, Avoiding room temperature storage and delayed cryopreservation provide better postthaw potency in hematopoietic progenitor cell grafts, Transfusion 53 (2013) 1834–1842, https://doi.org/10.1111/trf.12006.
[39] J.Y. Seo, H.-J. Huh, H.-K. Park, H.-K. Choung, D.-W. Kim, H.H. Koo, K.W. Sung, E.-S. Kang, Evaluation of overnight storage conditions for autologous peripheral blood stem cell products: comparison of three different conditions, Vox Sang. 103 (2012) 150–158, https://doi.org/10.1111/j.1423-0410.2012.01587.x.
[40] A. Jerram, T.V. Guy, L. Beutler, B. Gunasegaran, R. Sluyter, B. Fazekas St Groth, H. M. McGuire, Effects of storage time and temperature on highly multiparametric flow analysis of peripheral blood samples; implications for clinical trial samples, Biosci. Rep. 41 (2) (2021), https://doi.org/10.1042/BSR20203827. BSR20203827.
[41] M. Wojciuk, Z. Swiderska-Chadaj, K. Siwek, A. Gertych, Improving classification accuracy of fine-tuned CNN models: impact of hyperparameter optimization, Heliyon 10 (2024) e26586, https://doi.org/10.1016/j.heliyon.2024.e26586.
[42] R. Wangen, E. Aasebø, A. Trentani, S.-O. Døskeland, Ø. Bruserud, F. Selheim, M. Hernandez-Valladares, Preservation method and phosphate buffered saline washing affect the acute myeloid Leukemia proteome, Int. J. Mol. Sci. 19 (2018), https://doi.org/10.3390/ijms19010296.
[43] L. Zhu, M. Rajendram, K.C. Huang, Effects of fixation on bacterial cellular dimensions and integrity, iScience 24 (2021) 102348, https://doi.org/10.1016/j.isci.2021.102348.
[44] M. Sharifian Gh, F. Norouzi, Guidelines for an optimized differential centrifugation of cells, Biochem. Biophys. Rep. 36 (2023) 101585, https://doi.org/10.1016/j.bbrep.2023.101585.